Synthesis, Characterization and Photochromic Studies of Spirooxazine-Containing 2,2′-Bipyridine Ligands and Their Rhenium(I) Tricarbonyl Complexes

Chi-Chiu Ko, Li-Xin Wu, Keith Man-Chung Wong, Nianyong Zhu, and Vivian Wing-Wah Yam*[a]

Abstract: A series of spirooxazine-containing 2,2′-bipyridine ligands and their rhenium(I) tricarbonyl complexes has been designed and synthesized, and their photophysical, photochromic and electrochemical properties have been studied. The X-ray crystal structures of two of the complexes have been determined. Detailed studies showed that the emission properties of the complexes could readily be switched through photochromic reactions.

Keywords: luminescence · N ligands · photochromism · rhenium · spirooxazine

Introduction

The rapid expansion in the development of new optical memory and storage devices has inspired research into photochromic compounds, which are promising candidates as optical recording and storage materials,[1] and as materials for ophthalmic and sunglass lenses.[2] In addition to their potential applications utilizing their different absorption properties, the changes in electron delocalization have also been employed for the design of photoswitchable non-linear optical devices,[3] enzymatic systems,[4] host–guest systems[5] and luminescent devices.[6] Spirooxazines are one of the most popular classes of photochromic materials, and have been shown to possess high fatigue resistance and excellent photostability.[7] The photochromism of spirooxazines is attributable to the photochemical cleavage of the spiro-C–O bond, which results in the extension of π-conjugation in the colored photomerocyanine conformer and thus shifts the absorption to the visible region. It has been extensively studied and reviewed.[7b,8] Most studies of this class have been confined to the organic system, and it has not been until recently that increasing study of the incorporation of these organic spirooxazines/spiropyrans into transition metal complex systems[9] has been pursued. The incorporation of such photochromic moieties into transition metal complex systems would be expected to give rise to perturbation of the photochromic behavior. Gust et al., for example, showed that a spiropyran could be photosensitized by the excited state of a zinc–porphyrin system.[9a] In our previous communication, we have demonstrated the photosensitization of a pyridine-containing spirooxazine by the rhenium(I) tricarbonyl diimine complex system.[9b] As an extension of this work, a series of spirooxazine-containing 2,2′-bipyridine ligands and their rhenium(I) tricarbonyl complexes has been synthesized and characterized. The switching of their emission properties through photochromic reactions is also reported.

[a] Dr. C.-C. Ko, Dr. L.-X. Wu, Dr. K. M.-C. Wong, Dr. N. Zhu, Prof. Dr. V. W.-W. Yam
Centre for Carbon-Rich Molecular and Nano-Scale Metal-Based Materials Research
Department of Chemistry, and HKU-CAS Joint Laboratory on New Materials
The University of Hong Kong, Pokfulam Road, Hong Kong SAR (P. R. China)
Fax: (+852) 2857-1586
E-mail: wwyam@hku.hk

Supporting information for this article is available on the WWW under http://www.chemeurj.org/ or from the author.

Results and Discussion

Synthesis: The synthetic routes for the formation of the spirooxazine-containing ligands are summarized in Scheme 1. Esterification of 1,3,3-trimethyl-9′-hydroxyspiroindoline-naphthoxazine (SO) with 2,2′-bipyridine-4,4′-dicarboxylic acid[10] and the unsymmetrically substituted 2,2′-bipyridine, 4′-methyl-2,2′-bipyridine-4-carboxylic acid (prepared by the stepwise oxidation of 4,4′-dimethyl-2,2′-bipyridine with selenium(IV) dioxide and silver(I) oxide without isolation of the intermediates, as described by McCafferty et al.[11]) in the presence of triethylamine in anhydrous benzene at room temperature gave L1 and L2, respectively. Substitution reactions of mono- or di(bromomethyl)-substituted 2,2′-bipyri-

DOI: 10.1002/chem.200305485

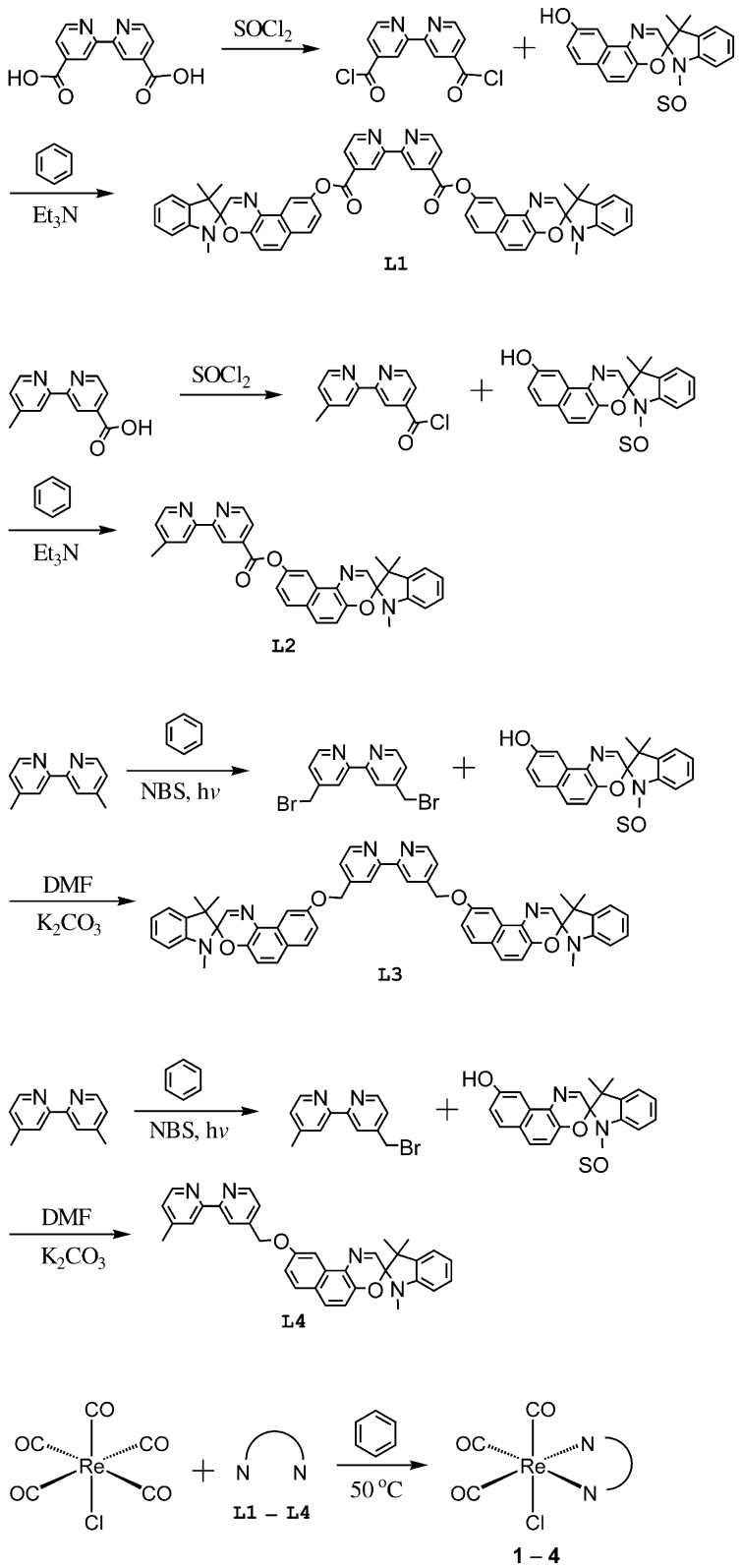

Scheme 1. Synthetic routes to spirooxazine-containing ligands and their rhenium(I) tricarbonyl complexes.

dines (prepared by bromination of 4,4′-dimethyl-2,2′-bipyridine with *N*-bromosuccinimide[12]) with SO in the presence of K_2CO_3 in DMF at room temperature gave L3 and L4. Substitution reactions of $[Re(CO)_5Cl]$ with the corresponding diimine ligands in anhydrous benzene at 50 °C afforded complexes **1**–**4**, which were isolated as yellow to red crystals, depending on the nature of the diimine ligands, after purification by column chromatography on silica gel and subsequent recrystallization from CH_2Cl_2/Et_2O. The identities of the ligands L1–L4 and complexes **1**–**4** were confirmed by satisfactory elemental analyses, ^{1}H NMR spectroscopy, IR spectroscopy and FAB mass spectrometry, and for complexes **1** and **2** also by X-ray crystallography.

X-ray crystal structure determination: Perspective drawings of complexes **1** and **2** are depicted in Figure 1 and Figure 2, respectively, the structure determination data are collected in Table 1, and selected bond lengths and angles are summarized in Table 2. The rhenium atom adopted a distorted octahedral geometry with the three carbonyl groups in a facial arrangement. The angles subtended by the nitrogen atoms of L1 and L2 at the rhenium centre, N1-Re1-N2, were 74.7° and 74.8°, respectively, which are much smaller than the ideal angle of 90° adopted in octahedral geometry. The deviation from the ideal angle is due to the steric requirement of the chelating ligands L1 and L2, which is commonly observed in other related complex systems.[13]

The average bond length of the spiro C–O moiety in **1** and **2** was about 1.47 Å, slightly longer than the typical length of a C–O bond (1.43 Å)[14] in other oxazine systems. This indicates the relative weakness of the bond and is also consistent with the rationale for the photochromic reaction to involve the cleavage of this spiro carbon–oxygen bond. In addition, the average interplanar angle between the indoline and naphthoxazine planes of **1** and **2** was found to be 88.2°, indicative of an essentially orthogonal arrangement. The orthogonal interplanar angle and the rela-

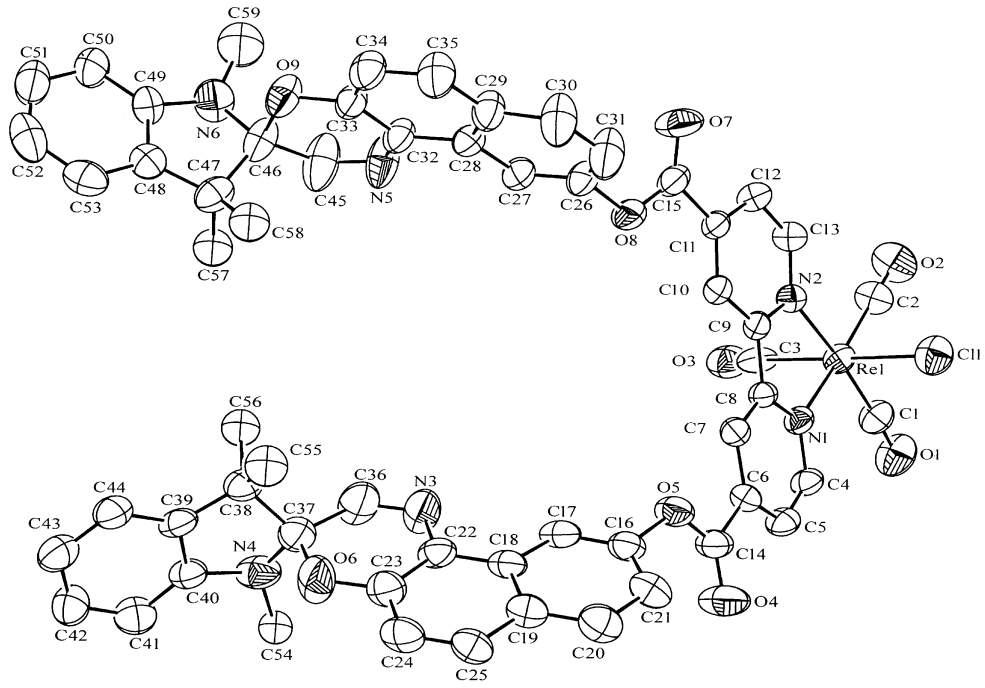

Figure 1. Structure of complex **1** with atomic numbering. Hydrogen atoms have been omitted for clarity. Thermal ellipsoids are shown at the 30% probability level.

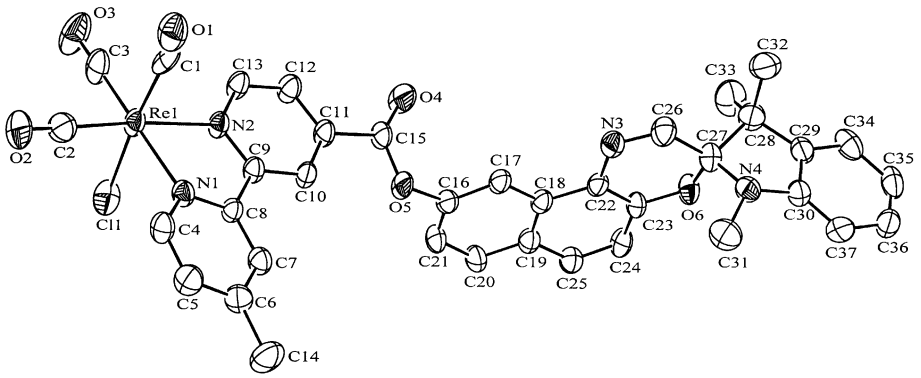

Figure 2. Structure of complex **2** with atomic numbering. Hydrogen atoms have been omitted for clarity. Thermal ellipsoids are shown at the 30% probability level.

tively longer spiro C–O bond length are also commonly observed in other related spiropyran[14a,b] and spirooxazine[14c–f] systems.

Electronic absorption spectroscopy: The photophysical data for all the ligands and complexes are collected in Table 3. The electronic absorption spectra of the free ligands in dichloromethane show very intense absorption bands, with molar extinction coefficients in the order of $10^4\,dm^3\,mol^{-1}\,cm^{-1}$ at about 280 and 300 nm, which are tentatively assigned as intraligand (IL) $\pi\rightarrow\pi^*$ transitions of the bipyridine and indoline moieties. The additional moderately intense bands and shoulders at about 330, 348 and 368 nm are most likely to be IL $\pi\rightarrow\pi^*$ transitions of the naphthoxazine moiety, similar to those observed in other related systems.[15] The assignments of these low-energy absorptions have been further supported by the observation that the values of the molar extinction coefficients from 330–380 nm in the ligands with two spirooxazine moieties (L1 and L3) are nearly twice those of ligands with one spirooxazine moiety (L2 and L4). Complexes **1**–**4**, on the other hand, in addition to the very intense IL absorptions at 300–365 nm, also each show a moderately intense band at about 400–440 nm in their electronic absorption spectra. This absorption band, with molar extinction coefficients in the order of $10^3\,dm^3\,mol^{-1}\,cm^{-1}$, is ascribed to the metal-to-ligand charge transfer (MLCT) [$d\pi(Re)\rightarrow\pi^*$(diimine)] transition, typical of rhenium(I) tricarbonyl diimine systems,[13,16] probably with some mixing of a ligand-centered character. An absorption energy dependence of this band, inversely related to the π-accepting ability of the bipyridine ligands, is observed (**3**$\approx$**4**$>$**2**$>$**1**), in agreement with the MLCT assignment. The observation of a very weak band at about 604 nm, both in the ligands and in the complexes, is attributable to the absorption of the open form, which is present in trace amounts and in thermal equilibrium with the closed form, as typically found in these systems.[7a,17]

Excitation of the ligands in solution in CH_2Cl_2 at room temperature at $\lambda > 350$ nm produces weak luminescence. Ligands L1 and L2 each show two emission bands at 438 and 530 nm, with the low-energy band being more prominent, while ligands L3 and L4 each show only one emission band,

Table 1. Crystal and structure determination data for complexes **1** and **2**.

	1	**2**
formula	$C_{59}H_{44}ClN_6O_9Re\cdot 2\,CH_2Cl_2\cdot 2\,H_2O$	$C_{37}H_{28}ClN_4O_6Re\cdot CHCl_3$
M_r	1408.54	965.65
T [K]	301	301
a [Å]	13.899(3)	12.039(2)
c [Å]	14.209(3)	12.503(3)
c [Å]	16.749(3)	13.461(3)
α [°]	105.64(3)	94.26(3)
β [°]	90.26(3)	95.68(3)
γ [°]	98.44(3)	110.43(3)
V [Å^3]	3147.3(11)	1876.5(6)
crystal color	red	yellowish orange
crystal system	triclinic	triclinic
space group	$P\bar{1}$ (no. 2)	$P\bar{1}$ (no. 2)
Z	2	2
$F(000)$	1416	952
ρ_{calcd} [g cm^{-3}]	1.486	1.709
crystal dimensions [mm]	0.50×0.30×0.20	0.50×0.20×0.10
λ [Å (graphite-monochromated, $Mo_{K\alpha}$)]	0.71073	0.71073
μ [cm^{-1}]	22.05	35.75
oscillation [°]	2	2
no. of images collected	100	77
distance [mm]	120	120
exposure time [s]	300	600
no. of data collected	15856	9405
no. of unique data	8143	5848
no. of data used in refinement [m]	6026	4878
no. of parameters refined [p]	751	478
R	0.0539	0.0428
wR[a]	0.1430	0.1213
residual extrema in final difference map [e Å^{-3}]	+0.958, −0.928	+0.563, −1.004

[a] $w = 1/[\sigma^2(F_o^2)+(aP)^2+bP]$, where $P = [2F_c^2\cdot\mathrm{Max}(F_o^2, 0)]/3$

Table 2. Selected bond lengths [Å] and bond angles [°] with estimated standard deviations (esds) in parentheses for **1** and **2**.

	1		
Re1–C1	1.905(10)	Re1–N2	2.168(6)
Re1–C2	1.916(11)	O6–C37	1.440(12)
Re1–C3	2.031(10)	O9–C46	1.459(12)
Re1–N1	2.163(6)		
C1-Re1-C2	88.4(4)	O6-C37-C38	107.7(9)
C1-Re1-C3	93.0(4)	N4-C37-C38	102.9(8)
C2-Re1-C3	93.1(4)	O9-C46-C47	111.2(8)
N1-Re1-N2	74.7(2)	N6-C46-C47	102.3(8)
	2		
Re1–C3	1.928(10)	Re1–N1	2.164(6)
Re1–C2	1.942(9)	Re1–N2	2.175(5)
Re1–C1	2.071(12)	O6–C27	1.455(9)
C3-Re1-C2	88.8(3)	N1-Re1-N2	74.7(2)
C3-Re1-C1	92.5(4)	O6-C27-C26	111.0(6)
C2-Re1-C1	88.9(4)	N4-C27-C28	101.5(6)

at 450 nm. With reference to previous related spectroscopic works,[9c,d] the low-energy emission band at about 530 nm, only observed in ligands L1 and L2, is tentatively assigned as ligand-centered phosphorescence while the high-energy band at about 440–450 nm found in all the ligands studied is tentatively assigned as ligand-centered fluorescence. On the other hand, excitation of complexes **1**–**4** in CH_2Cl_2 solutions at $\lambda > 400$ nm at room temperature resulted in strong luminescence (Figure 3), with emission maxima at about 633–722 nm, depending on the nature of the diimine ligand. This emission band is assigned as deriving from a ^{3}MLCT [dπ(Re)→π*(diimine)] origin, probably mixed with some ^{3}LC character. The emission energy dependence—**3** ≈ **4** (633 nm) > **2** (695 nm) > **1** (722 nm)—is inversely related to the π-accepting ability of the diimine ligands—L1 > L2 > L4 ≈ L3—and in agreement with such a ^{3}MLCT origin. The MLCT emission energy of **1** was found to be the lowest of the complexes studied, and is in accord with the strongest π-accepting ability of L1 in complex **1**. Similarly, with poorer π-accepting diimine ligands, such as L3 and L4 in complexes **3** and **4**, higher-energy emission bands were observed. Complexes **1** and **2** also display strong photoluminescence in EtOH/MeOH/CH_2Cl_2 (4:1:1 v/v/v) glass at 77 K, while complexes **3** and **4** are found to be non-emissive in this medium. These emissions are also tentatively assigned as ^{3}MLCT phosphorescence, probably mixed with some ^{3}LC character, similar to that observed in solution at room temperature.

Upon excitation at 365 nm, the ligands and the complexes exhibit photochromism, with a growth in intensity of the band at 604 nm, corresponding to the generation of the open form. The open form generated is thermally unstable and readily undergoes thermal bleaching, which follows first order kinetics, to the closed form. Unlike the previously reported[9c] rhenium complexes—$[Re(N–N)(CO)_3(SOPY)]^+$ (SOPY = 1,3,3-trimethylspiroindolinenaphthoxazine-9′-yl nicotinate)—however, complexes **1**–**4** did not show photochromism with MLCT (400–440 nm) excitation. This is probably because the energies of the ^{3}MLCT excited state of the complexes, which are estimated to be about 166–188 kJ mol^{-1} from the phosphorescence of the complexes (633–722 nm), are insufficient for sensitization when compared to the triplet excited state energies of spirooxazines (≈210–225 kJ mol^{-1}).[18]

Excitation of L1–L4 and complexes **1**–**4** at 365 nm in dry ice/acetone baths at 195 K converted the closed forms of the ligands and their complexes to the open forms, photomerocyanine, and slowed down the thermal bleaching reactions. Figure 4 shows the emission spectra of complexes **1** and **2** as well as their open forms in EtOH/MeOH/CH_2Cl_2 (4:1:1 v/v/v) at 77 K. The original emission band associated with the closed forms of complexes **1** and **2** disappeared, with the evolution of a new emission band, peaking at 705–710 nm, corresponding to the emission of the open forms of the complexes. On the other hand, excitation of the open forms of L1–L4 and complexes **3** and **4**, which, unlike their closed forms, are non-emissive in this medium, shows emission bands at 705–710 nm. In view of the close resemblance of the emissions of the open forms of the complexes to those of the free ligands and the relative insensitivity of the emis-

Table 3. Photophysical data for the ligands and the complexes.

	Absorption λ_{abs}[a] [nm] (ε [$dm^3 mol^{-1} cm^{-1}$])	Medium (T [K])	Emission λ_{em}[b] [nm] (τ_o [μs])
L1	302(30880), 316(26960), 346(10310), 368(5620)	CH_2Cl_2 (298)	438 (<0.1), 530 (<0.1)
		glass[c] (77)	–[d]
L1(PMC)		glass[c] (77)	710 (0.5)
L2	284(19590), 304(16260), 316(14370), 346(5170), 368(2810)	CH_2Cl_2 (298)	438 (<0.1), 530 (<0.1)
		glass[c] (77)	–[d]
L2(PMC)		glass[c] (77)	710 (0.8)
L3	276(28310), 334(15660), 348(13720)	CH_2Cl_2 (298)	445 (<0.1)
		glass[c] (77)	–[d]
L3(PMC)		glass[c] (77)	705 (0.8)
L4	280(22230), 334(8720), 348(7670)	CH_2Cl_2 (298)	445 (<0.1)
		glass[c] (77)	–[d]
L4(PMC)		glass[c] (77)	705 (0.9)
1	320(22920), 344(12590), 360(8780), 374(5280), 440(3900)	CH_2Cl_2 (298)	722 (<0.1)
		glass[c] (77)	642 (1.9)
1(PMC)		glass[c] (77)	710 (1.8)
2	306(21750), 316(21080), 346(7790), 364(5770), 416(4760)	CH_2Cl_2 (298)	695 (<0.1)
		glass[c] (77)	600 (3.5)
2(PMC)		glass[c] (77)	710 (2.7)
3	294(33820), 316(19690), 334(14660), 346(13120), 400(4690)	CH_2Cl_2 (298)	633 (<0.1)
		glass[c] (77)	–[d]
3(PMC)		glass[c] (77)	705 (<0.1)
4	294(22650), 316(13260), 334(9930), 346(8920), 398(3310)	CH_2Cl_2 (298)	633 (<0.1)
		glass[c] (77)	–[d]
4(PMC)		glass[c] (77)	705 (<0.1)

[a] In dichloromethane at 298 K. [b] Excitation wavelength at ca. 420 nm. Emission maxima are corrected values. [c] EtOH/MeOH/CH_2Cl_2 (4:1:1, v/v/v). PMC: photomerocyanine form. [d] Non-emissive.

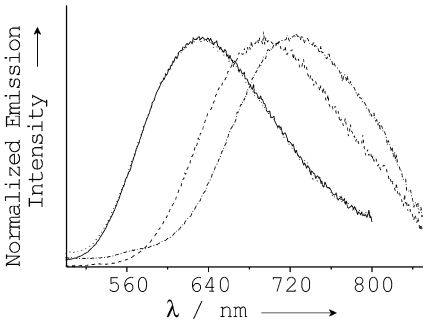

Figure 3. Normalized solution emission spectra of **1** (–•–•), **2** (– – –), **3** (——) and **4** (•••••) in dichloromethane at 298 K.

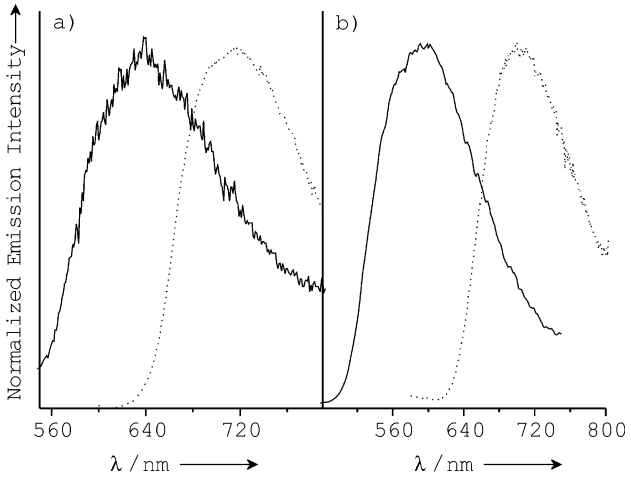

Figure 4. Normalized emission spectra of the closed forms (——) and the open forms (•••••) of **1** (a) and **2** (b) in EtOH/MeOH/CH_2Cl_2 (4:1:1 v/v/v) at 77 K.

sion energies to the nature of the bipyridine ligands, the emission is assigned as LC emission, probably originating from the LC phosphorescence of the photomerocyanine form of the spironaphthoxazine moiety. Similar assignments have also been reported in the literature.[18b]

Bleaching reaction kinetics: The kinetics for the bleaching reactions of the photomerocyanines of the ligands L1, L2 and L4 and complexes **1–4**, after excitation at 365 nm, were investigated in acetonitrile solution. Figure 5 shows representative UV/Vis spectral changes in the photomerocyanines with time, together with the absorbance trace at λ_{max} = 604 nm as a function of time. The thermodynamic activation parameters are collected in Table 4. The activation enthalpies for the reactions of the ligands L1, L2, and L4 are found to be 45–70 $kJ mol^{-1}$, which are in a range typical of those reported for this type of compounds in the literature,[19] while their activation entropies vary much more drastically, from $-17.7 J mol^{-1} K^{-1}$ when $\Delta H^{\neq}$ is large to $-100.3 J mol^{-1} K^{-1}$ when $\Delta H^{\neq}$ is small, as has been discussed in the literature.[15,19] The positive values for the activation enthalpies indicated that the bleaching reaction is an activated process. The orderness in the activated complex in the transition state in relation to the open form is decreased, as reflected in the negative values of the activation entropies.

The activation enthalpies and entropies for the reactions in complexes **1–4** range from 54.8 to 60.5 $kJ mol^{-1}$ and from -47.8 to $-66.9 J mol^{-1} K^{-1}$, respectively. The variations in the activation enthalpy and entropy in these complexes are

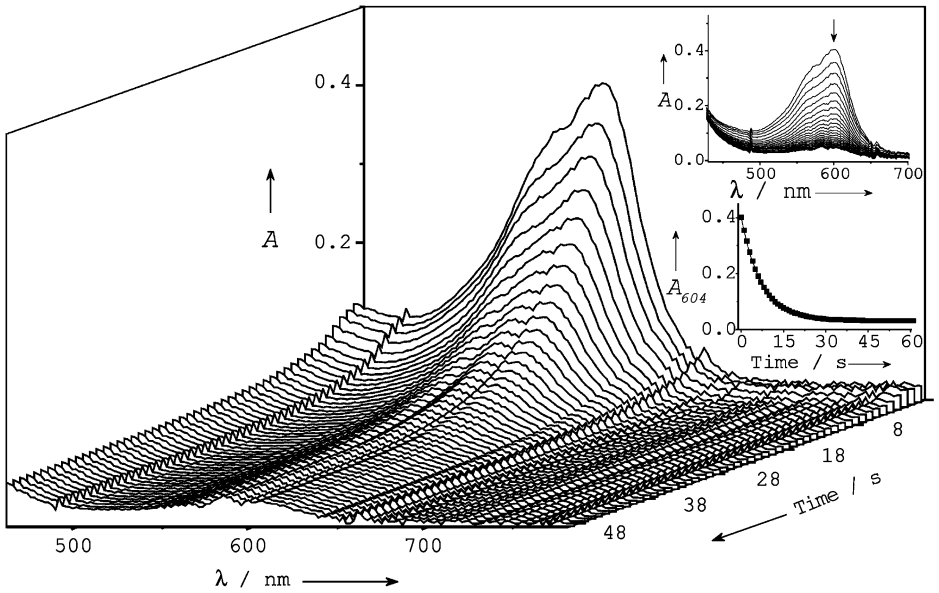

Figure 5. Time-dependent UV/Vis absorption spectral changes in the open form of complex **3** in CH_3CN at 5.6 °C after excitation at 365 nm. The inserts show the overlaid UV/Vis absorption spectra at different decay times and the decay trace at the absorption maximum at 604 nm with time.

Table 4. Activation parameters for the bleaching reaction of the ligands and the complexes in solution in acetonitrile.

	$\Delta H^{\neq}$ [kJ mol^{-1}]	$\Delta S^{\neq}$ [J^{-1} mol^{-1} K^{-1}]	E_a [kJ mol^{-1}]
L1	45.0 ± 0.9	−100.3 ± 3.3	47.3 ± 0.9
L2	69.1 ± 2.8	−17.7 ± 9.1	71.5 ± 2.8
L3	_[a]	_[a]	_[a]
L4	57.3 ± 3.3	−57.3 ± 11.6	59.6 ± 3.3
1	60.5 ± 3.2	−47.8 ± 11.1	62.9 ± 3.2
2	54.8 ± 2.2	−66.9 ± 7.7	57.1 ± 2.2
3	58.5 ± 1.7	−51.5 ± 5.9	60.9 ± 1.7
4	57.6 ± 3.2	−53.6 ± 11.3	59.0 ± 3.2

[a] Data not obtained, due to the insolubility of the compound.

much smaller than those in their free ligands. A relationship between $\Delta H^{\neq}$ and $\Delta S^{\neq}$ similar to that seen in the free ligands and discussed in the literature,[15,19] has also been observed in the complexes, although the extent of the variation is much smaller. The range of activation energies (E_a) for these complexes also changes much less significantly, from 57.1 to 62.9 kJ mol^{-1}, as compared to those of the free ligands, which range from 47.3 to 71.5 kJ mol^{-1}. A careful investigation on the variation between $\Delta H^{\neq}$ and $\Delta S^{\neq}$ in the whole series of complexes **1**–**4** and their free ligands L1, L2 and L4 has been performed. An isokinetic relationship—that is, a linear proportionality between $\Delta H^{\neq}$ and $\Delta S^{\neq}$, as shown in the plot of $\Delta H^{\neq}$ and $\Delta S^{\neq}$ (Figure 6)—has been obtained. This is indicative of a common bleaching reaction mechanism for the whole series of complexes and the ligands. From the slope of the plot, an isokinetic temperature of 285.0 ± 3.9 K for the bleaching reaction is obtained.

Photochemical quantum yield for the photochromic reaction (Table 5): The quantum yields for the spirooxazine-containing bipyridine ligands with excitation at $\lambda = 365$ nm are in the range of 0.36–0.60. The increased efficiency of complex **4** in relation to its free ligand L4 may be a result of the presence of the heavy rhenium atom, which enhances the spin–orbit coupling and hence improves the intersystem crossing efficiency through the relaxation of spin-forbidden processes, resulting in a more allowed and efficient ring-opening reaction to produce the photomerocyanine via the triplet state. Although the triplet pathway would be much enhanced in the presence of the heavy atom, the quantum efficiencies for complexes **1** and **2** in relation to those of their free ligands L1 and L2, respectively, are found to be decreased. It is likely that the lower quantum efficiencies of **1** and **2** than those of their free ligands are attributable to the presence of low-lying

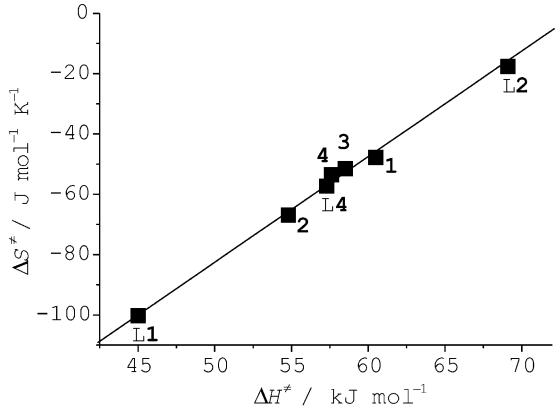

Figure 6. A plot of activation enthalpy against activation entropy for the bleaching reactions of the open forms of the ligands L1, L2 and L4 and the complexes **1**–**4**.

^{3}MLCT states in these complexes, which would provide an efficient quenching pathway for the triplet state of the spirooxazine moiety, and thus decrease the efficiency for the photochromic reaction via the triplet pathway.

Table 5. A summary of the estimated photochemical quantum yields of the photochromic forward reactions of the ligands and the complexes in acetonitrile with excitation at $\lambda = 365$ nm.

	ϕ_{365}
L1	0.60 ± 0.01
L2	0.45 ± 0.01
L3	_[a]
L4	0.44 ± 0.01
1	0.15 ± 0.01
2	0.18 ± 0.01
3	0.48 ± 0.01
4	0.65 ± 0.01

[a] Data were not obtained, due to the insolubility of the compound.

The quantum efficiencies for the photochromic reactions of the complexes are in the order **4** (0.65) > **3** (0.48) > **2** (0.18) > **1** (0.15), in accord with the energies of the MLCT excited states. This trend is supportive of the quenching mechanism (from the triplet state of spirooxazine to ^{3}MLCT), in which the efficiency of the quenching pathway increases as the ^{3}MLCT excited state energy decreases.

Electrochemical studies: Complexes **1**–**4** each display an irreversible oxidation wave at about +0.91 to +0.99 V, and a quasi-reversible oxidation couple at about +1.28 to +1.40 V in the oxidative scan of their cyclic voltammograms in acetonitrile (0.1 mol dm^{-3} nBu$_4$NPF$_6$), while two to three quasi-reversible reduction couples and one irreversible reduction wave at −0.90 to −2.02 V versus SCE are observed in the reductive scan. Complexes **3** and **4** also each show an irreversible oxidation wave at about +1.76 V. The electrochemical data for the free ligands and their rhenium(I) complexes are summarized in Table 6.

Table 6. Electrochemical data for the ligands and the complexes in acetonitrile solution (0.1 mol dm^{-3} nBu$_4$NPF$_6$) at 298 K[a].

Compound	Oxidation[b] $E_{1/2}$ [V] vs. SCE (E_{pa} [V] vs. SCE)	Reduction[b] $E_{1/2}$ [V] vs. SCE (E_{pc} [V] vs. SCE)
L1	–[c]	–[c]
L2	(+1.03)	−1.68, −2.12
L3	–[c]	–[c]
L4	(+0.93), +1.70	(−2.06), (−2.19)
1	(+0.99), +1.40	−0.92, (−1.28), −1.44, −1.96
2	(+0.99), +1.34	−1.08, −1.55, −1.99
3	(+0.91), +1.29, (+1.76)	−1.33, −1.59, (−1.85), −2.01
4	(+0.91), +1.28, (+1.76)	(−1.44), −1.49, (−1.81), −2.02

[a] Working electrode, glassy carbon; scan rate, 100 mV s^{-1}. [b] $E_{1/2}$ is (E_{pa} + E_{pc})/2; E_{pa} and E_{pc} are peak anodic and peak cathodic potentials, respectively. [c] Data could not be obtained, due to the low solubility of the compound in acetonitrile solution (0.1 mol dm^{-3} nBu$_4$NPF$_6$).

With reference to previous electrochemical studies on related indolinespiropyrans[20] and indolinespirooxazines,[21] as well as the close resemblance of the potentials of the first irreversible oxidation wave to those of the corresponding free ligands, the first oxidative wave is assigned to the oxidation of the spirooxazine moiety, probably arising from the removal of a lone-pair electron on the nitrogen atom of the indoline moiety. The more positive potential of this oxidation wave in complexes **1** and **2** (ca. +0.99 V vs. SCE) and L2 (ca. +1.03 V vs. SCE) than in complexes **3** and **4** (ca. +0.91 V vs. SCE) and L4 (ca. +0.93 V vs. SCE) is supportive of a spirooxazine ligand-centered oxidation, since the presence of the electron-withdrawing ester linkage in L2 and hence complexes **1** and **2** would render the oxidation process more difficult.

The second quasi-reversible oxidation couple in the rhenium complexes, at about +1.28 to +1.40 V, is found to be dependent on the nature of the diimine ligand and is assigned to the metal-centered oxidation of Re^{I} to Re^{II}. The potential for the oxidation is found to follow the order: **1** (+1.40 V) > **2** (+1.34 V) > **3** (+1.29 V) > **4** (+1.28 V), in line with the π-accepting ability of the diimine ligands: L1 > L2 > L3 > L4. In general, the better the π-accepting ability of the diimine ligand, the more stable the dπ(Re) orbital will be, and hence the more difficult the oxidation process. Similar oxidation couples ascribed to a Re^{I}Re^{II} oxidation have been reported in other related systems, Re(CO)$_3$(N–N)Cl.[22]

The third irreversible oxidation wave, which occurs at about +1.76 V, is only observable in complexes **3** and **4**. The close resemblance of this oxidation wave to that observed in the free ligand L4 is suggestive of a ligand-centered oxidation. The slightly more positive potential in complex **4** than in its free ligand L4 is probably attributable to the electron-withdrawing effect of the rhenium metal centre upon coordination.

The first two reduction couples are tentatively assigned to the bipyridyl ligand-centered reductions, as they are commonly observed in related systems.[20,21] The trends of these reduction potentials are also in line with the electron-richness and π-accepting ability of the diimine ligands as discussed earlier, while the other two, more negative reductions are assigned to the ligand-centered reduction of the spirooxazine moiety, as similar waves are observed in the free ligand reductions. In general, coordination of the ligands to the rhenium metal centre should render the ligand less electron-rich and thus make the ligand-centered reductions in the complexes more ready to occur. As a result, potentials less negative than seen in the free ligands are commonly observed in the complexes.

Conclusion

A series of spirooxazine-containing 2,2′-bipyridine ligands has been successfully synthesized and incorporated into rhenium(I) tricarbonyl diimine complex systems. The moderately intense absorption at 400–440 nm in the complexes, which is absent in the absorption spectra of the free ligands, is assigned as the MLCT [dπ(Re)→π*(diimine)] transition, probably mixed with some LC character. All complexes exhibit strong ^{3}MLCT phosphorescence at 633–722 nm in CH_2Cl_2 at 298 K. However, in EtOH/MeOH/CH_2Cl_2 glass at 77 K, only complexes **1** and **2** display strong ^{3}MLCT emissions at about 642 nm and 600 nm, respectively, and this emission band would be switched to LC phosphorescence of photomerocyanine moiety at 705–710 nm upon conversion to the open form.

The activation parameters for the thermal bleaching reactions have been determined. The activation enthalpies for ligands L1, L2 and L4 are 45–70 kJ mol^{-1} and the activation entropies for the ligands L1, L2 and L4 vary drastically from −17.7 J mol^{-1} K^{-1} when $\Delta H^{\neq}$ is large to −100.3 J mol^{-1} K^{-1} when $\Delta H^{\neq}$ is small. A similar relationship between $\Delta H^{\neq}$ and $\Delta S^{\neq}$ has also been observed in the complexes, but the extent of the variation is much smaller. The variations in the activation enthalpy, activation entropy and the activation energy in all the complexes are also much smaller than those in the free ligands. An isokinetic relationship, with an isokinetic temperature of 285.0 ± 3.9 K, has been obtained for the bleaching reactions.

Experimental Section

Materials and reagents: $[Re(CO)_5Cl]$ was obtained from Strem Chemicals, Inc. 4,4′-Dimethyl-2,2′-bipyridine and *N*-bromosuccinimide were obtained from Aldrich Chemical Co. 2,2′-Bipyridine-4,4′-dicarboxylic acid was prepared by a slight modification of a reported procedure.[10] 4,4′-Di(bromomethyl)-2,2′-bipyridine ($(BrCH_2)_2$bpy)) and 4-bromomethyl-4′-methyl-2,2′-bipyridine were prepared by slight modifications of a reported procedure.[12] 4′-Methyl-2,2′-bipyridine-4-carboxylic acid was prepared by a slight modification of a reported procedure.[11] 1,3,3-Trimethyl-9′-hydroxy-spiroindolinenaphthoxazine (SO) was synthesized by modification of a reported procedure.[23] Benzene (Lab-Scan, AR) was distilled over sodium before use for synthesis. All other reagents were of analytical grade and were used as received.

Syntheses

Bis(1,3,3-trimethylspiroindolinenaphthoxazine-9′-yl) 2,2′-bipyridyl-4,4′-dicarboxylate (L1): 2,2′-Bipyridyl-4,4′-dicarboxylic acid chloride was freshly prepared by heating 2,2′-bipyridyl-4,4′-dicarboxylic acid (130 mg, 0.61 mmol) at reflux with thionyl chloride (15 mL) until a clear solution was obtained. The excess thionyl chloride was removed under reduced pressure at room temperature to leave a white solid consisting of the acid chloride. Benzene (20 mL), triethylamine (5 mL) and SO (2.0 equivalents, 420 mg, 1.22 mmol) were then added to the freshly prepared acid chloride. The resulting mixture was then stirred at room temperature for two days. After removal of the solvent under reduced pressure and at room temperature, the residue was purified by column chromatography on silica gel with chloroform/diethyl ether (8:1 v/v) as eluent to afford **1** as a white solid. Yield: 208 mg, 0.23 mmol; 38%. ^{1}H NMR (300 MHz, $CDCl_3$, 298 K): δ = 1.37 (s, 12H; –Me), 2.78 (s, 6H; –NMe), 6.59 (d, J = 7.6 Hz, 2H; indolinic proton at 7-position), 6.91 (t, J = 7.6 Hz, 2H; indolinic proton at 5-position), 7.04 (d, J = 8.9 Hz, 2H; naphthoxazinic proton at 5′-position), 7.10 (d, J = 7.6 Hz, 2H; indolinic proton at 4-position), 7.23 (t, J = 7.6 Hz, 2H; indolinic proton at 6-position), 7.32 (dd, J = 2.3 Hz, 8.9 Hz, 2H; naphthoxazinic proton at 8′-position), 7.71 (d, J = 8.9 Hz, 2H; naphthoxazinic proton at 6′-position), 7.83 (s, 2H; naphthoxazinic proton at 2′-position), 7.85 (d, J = 8.9 Hz, 2H; naphthoxazinic proton at 7′-position), 8.13 (d, J = 4.9 Hz, 2H; bipyridyl proton at 5,5′-position), 8.44 (d, J = 2.3 Hz, 2H; naphthoxazinic proton at 10′-position), 9.00 (d, J = 4.9 Hz, 2H; bipyridyl proton at 6,6′-position), 9.24 ppm (s, 2H; bipyridyl proton at 3,3′-position); IR (KBr disc): $\tilde{\nu}$ = 1750 cm^{-1} (C=O); positive ion FAB-MS: m/z: 897 $[M+H]^+$; elemental analyses calcd (%) for $C_{56}H_{44}N_6O_6$ (897): C 74.98, H 4.94, N 9.34; found: C 74.66, H 5.17, N 8.94.

1,3,3-Trimethylspiroindolinenaphthoxazine-9′-yl 4′-methyl-2,2′-bipyridyl-4-carboxylate (L2): The title ligand was synthesized by a procedure similar to that used for **1**, except that 4′-methyl-2,2′-bipyridyl-4-carboxylic acid was used in place of 2,2′-bipyridyl-4,4′-dicarboxylic acid, and 1 equivalent of SO (210 mg, 0.61 mmol) was used instead. Column chromatography on silica gel (230–400 mesh) with chloroform/diethyl ether (3:1 v/v) as eluent gave **2** as a white solid. Yield: 168 mg, 0.31 mmol; 51%. ^{1}H NMR (300 MHz, $CDCl_3$, 298 K): δ = 1.29 (s, 6H; –Me), 2.42 (s, 3H; –Me on 2,2′-bpy), 2.71 (s, 3H; –NMe), 6.53 (d, J = 7.8 Hz, 1H; indolinic proton at 7-position), 6.83 (t, J = 7.4 Hz, 1H; indolinic proton at 5-position), 6.98–7.05 (m, 2H; naphthoxazinic proton at 5′-position and indolinic proton at 4-position), 7.11–7.17 (m, 2H; indolinic proton at 6-position and bipyridyl proton at 5′-position), 7.24 (dd, J = 2.3 Hz, 8.8 Hz, 1H; naphthoxazinic proton at 8′-position), 7.69 (d, J = 8.8 Hz, 1H; naphthoxazinic proton at 6′-position), 7.70 (s, 1H; naphthoxazinic proton at 2′-position), 7.81 (d, J = 8.8 Hz, 1H; naphthoxazinic proton at 7′-position), 7.98 (dd, J = 1.6 Hz, 4.9 Hz, 1H; bipyridyl proton at 5-position), 8.29 (s, 1H; bipyridyl proton at 3′-position), 8.36 (d, J = 2.3 Hz, 1H; naphthoxazinic proton at 10′-position), 8.52 (d, J = 4.9 Hz, 1H; bipyridyl proton at 6′-position), 8.85 (d, J = 4.9 Hz, 1H; naphthoxazinic proton at 6-position), 9.10 ppm (d, J = 4.9 Hz, 1H; bipyridyl proton at 3-position); IR (KBr disc): $\tilde{\nu}$ = 1750 cm^{-1} (C=O); positive ion FAB-MS: m/z: 541 $[M+H]^+$; elemental analyses calcd (%) for $C_{34}H_{28}N_4O_3\cdot{}^1/_2\,H_2O$ (549): C 74.30, H 5.32, N 10.19; found: C 74.21, H 5.25, N 10.14.

4,4′-Bis(1,3,3-trimethylspiroindolinenaphthoxazine-9′-oxymethyl)-2,2′-bipyridine (L3): SO (2.0 equivalents, 570 mg, 1.65 mmol) was added to a stirred mixture of 4,4′-di(bromomethyl)-2,2′-bipyridine (280 mg, 0.82 mmol) and K_2CO_3 (250 mg, 1.78 mmol) in DMF (20 mL), and the mixture was stirred for two days. The reaction mixture was poured into deionized water (50 mL) to precipitate the crude product, which was then filtered and washed with copious amounts of deionized water. The crude product was then purified by column chromatography on silica gel with dichloromethane/diethyl ether (1:1 v/v) as eluent to give **3** as an analytically pure white powder. Yield: 70 mg, 0.08 mmol; 10%. ^{1}H NMR (300 MHz, CD_2Cl_2, 298 K): δ = 1.28 (s, 12H; –Me), 2.69 (s, 6H; –NMe), 5.35 (s, 4H; –Me on 2,2′-bipyridine), 6.51 (d, J = 7.7 Hz, 2H; indolinic proton at 7-position), 6.79–6.84 (m, 4H; naphthoxazinic proton at 5′-position and indolinic proton at 5-position), 7.02 (d, J = 7.2 Hz, 2H; indolinic proton at 4-position), 7.10–7.16 (m, 4H; naphthoxazinic proton at 8′-position and indolinic proton at 6-position), 7.46 (d, J = 5.0 Hz, 2H; bipyridyl proton at 5,5′-position), 7.57 (d, J = 8.8 Hz, 2H; naphthoxazinic proton at 6′-position), 7.65 (d, J = 8.8 Hz, 2H; naphthoxazinic proton at 7′-position), 7.67 (s, 2H; naphthoxazinic proton at 2′-position), 7.95 (d, J = 2.5 Hz, 2H; naphthoxazinic proton at 10′-position), 8.57 (s, 2H; bipyridyl proton at 3,3′-position), 8.66 ppm (d, J = 5.0 Hz, 2H; bipyridyl proton at 6,6′-position); positive ion FAB-MS: m/z: 869 $[M+H]^+$; elemental analyses calcd (%) for $C_{56}H_{48}N_6O_4\cdot H_2O$ (887): C 75.83, H 5.68, N 9.47; found: C 76.10, H 5.48, N 9.21.

4-(1,3,3-Trimethylspiroindolinenaphthoxazine-9′-oxymethyl)-4′-methyl-2,2′-bipyridine (L4): The title ligand was synthesized by a procedure similar to that used for **3**, except that 4-bromomethyl-4′-methyl-2,2′-bipyridine was used in place of 4,4′-di(bromomethyl)-2,2′-bipyridine, and 1 equivalent of SO (285 mg, 0.83 mmol) was used instead. Purification by column chromatography on silica gel with dichloromethane/diethyl ether (5:1 to 1:3 v/v) as eluent gave **4** as an analytically pure white powder. Yield: 106 mg, 0.2 mmol; 25%. ^{1}H NMR (300 MHz, CD_2Cl_2, 298 K): δ = 1.35 (s, 6H; –Me), 2.45 (s, 3H; –Me on bpy), 2.76 (s, 3H; –NMe), 5.38 (s, 2H; –OCH_2– on bpy), 6.57 (d, J = 7.5 Hz, 1H; indolinic proton at 7-position), 6.85–6.91 (m, 2H; naphthoxazinic proton at 5′-position and indolinic proton at 5-position), 7.08 (d, J = 7.1 Hz, 1H; indolinic proton at 4-position), 7.19–7.25 (m, 3H; naphthoxazinic proton at 8′-position, indolinic proton at 6-position and bipyridyl proton at 5′-position), 7.48 (d, J = 4.9 Hz, 1H; bipyridyl proton at 5-position), 7.59 (d, J = 8.8 Hz, 1H; naphthoxazinic proton at 6′-position), 7.68 (d, J = 8.8 Hz, 1H; naphthoxazinic proton at 7′-position), 7.71 (s, J = 7.1 Hz, 1H; naphthoxazinic proton at 2′-position), 7.98 (d, J = 2.1 Hz, 1H; naphthoxazinic proton at 10′-position), 8.26 (s, 1H; bipyridyl proton at 3′-position), 8.56 (m, 2H; bipyridyl proton at 3,6′-position), 8.71 ppm (d, J = 4.9 Hz, 1H; bipyridyl proton at 6-position); positive ion FAB-MS: m/z: 527 $[M+H]^+$; elemental analyses calcd (%) for $C_{34}H_{30}N_4O_2$ (526): C 77.54, H 5.74, N 10.64; found: C 77.59, H 5.89, N 10.54.

$[Re(CO)_3(L1)Cl]$ (1): The complex was prepared by a modification of a literature method used for the related Re^I diimine complexes.[24] $[Re(CO)_5Cl]$ (150 mg, 0.42 mmol) and L1 (407 mg, 0.44 mmol) were suspended in benzene (50 mL). The suspension was stirred at 45–50 °C under nitrogen for two days, during which the starting materials dissolved gradually to give a dark red solution, which subsequently changed to a red suspension. After removal of the solvent under reduced pressure, the residue was purified by column chromatography with dichloromethane/acetone (5:2 v/v) as eluent. Red crystals of **1** were obtained by slow diffusion of *n*-hexane vapor into a dichloromethane solution of the complex. Yield: 167 mg, 0.14 mmol; 33%. ^{1}H NMR (300 MHz, $CDCl_3$, 298 K): δ = 1.35 (s, 12H; –Me), 2.76 (s, 6H; –NMe), 6.58 (d, J = 7.7 Hz, 2H; indolinic proton at 7-position), 6.91 (t, J = 7.5 Hz, 2H; indolinic proton at 5-position), 7.04–7.10 (m, 4H; indolinic proton at 4-position and naphthoxazinic proton at 5′-position), 7.19–7.30 (m, 4H; indolinic proton at 6-position and naphthoxazinic proton at 8′-position), 7.69–7.74 (m, 4H; naphthoxazinic proton at 2′,6′-position), 7.86 (d, J = 8.9 Hz, 2H; naphthoxazinic proton at 7′-position), 8.34 (d, J = 5.7 Hz, 2H; bipyridyl proton at 5,5′-position), 8.45 (d, J = 2.4 Hz, 2H; naphthoxazinic proton at 10′-position), 9.09 (s, 2H; bipyridyl proton at 3,3′-position), 9.36 ppm (d, J = 5.7 Hz, 2H; bipyridyl proton at 6,6′-position); IR (KBr disc): $\tilde{\nu}$ = 1902, 1927, 2026 cm^{-1} (C=O), 1749 cm^{-1} (C=O); positive ion FAB-MS: m/z: 1202 $[M+H]^+$; elemental analyses calcd (%) for $C_{59}H_{44}ClN_6O_9Re\cdot{}^1/_4\,CH_2Cl_2$ (1224): C 58.14, H 3.64, N 6.87; found: C 58.00, H 3.93, N 6.65.

$[Re(CO)_3(L2)Cl]$ (2): The title complex was synthesized by a procedure similar to that used for **1**, except that L2 (245 mg, 0.44 mmol) was used in

place of L1 in the substitution reaction and dichloromethane/acetone (9:1 v/v) was used as eluent in the column chromatography. Slow diffusion of diethyl ether vapor into a concentrated $CHCl_3$ solution of the complex gave **2**, isolated as bright orange crystals. Yield: 181 mg, 0.21 mmol; 51 %. ^{1}H NMR (500 MHz, CD_2Cl_2, 298 K): δ = 1.36 (s, 6H; –Me), 2.62 (s, 3H; –Me on bpy), 2.77 (s, 3H; –NMe), 6.59 (d, J = 7.8 Hz, 1H; indolinic proton at 7-position), 6.89 (t, J = 7.6 Hz, 1H; indolinic proton at 5-position), 7.08–7.11 (m, 2H; naphthoxazinic proton at 5′-position and indolinic proton at 4-position), 7.21 (t, J = 7.6 Hz, 1H; indolinic proton at 6-position), 7.31 (dd, J = 2.4 Hz, 8.8 Hz, 1H; naphthoxazinic proton at 8′-position), 7.45 (d, J = 5.6 Hz, 1H; bipyridyl proton at 5′-position), 7.76 (d, J = 7.2 Hz, 1H; naphthoxazinic proton at 6′-position), 7.78 (s, 1H; naphthoxazinic proton at 2′-position), 7.89 (d, J = 8.8 Hz, 1H; naphthoxazinic proton at 7′-position), 8.26–8.27 (m, 2H; bipyridyl proton at 5,3′-position), 8.45 (d, J = 2.4 Hz, 1H; naphthoxazinic proton at 10′-position), 8.90 (d, J = 5.6 Hz, 1H; bipyridyl proton at 6′-position), 8.94 (s, 1H; bipyridyl proton at 3-position), 9.28 ppm (d, J = 5.6 Hz, 1H; bipyridyl proton at 6-position); IR (KBr disc): $\tilde{\nu}$ = 1881, 1926, 2024 cm^{-1} (C≡O), 1747 cm^{-1} (C=O); positive ion FAB-MS: m/z: 847 $[M+H]^+$, 811 $[M-Cl]^+$; elemental analyses calcd (%) for $C_{37}H_{28}ClN_4O_6Re\cdot CHCl_3$ (966): C 47.25, H 3.03, N 5.80; found: C 47.33, H 3.03, N 5.80.

[Re(CO)$_3$(L3)Cl] (3): The title complex was synthesized by a procedure similar to that used for **1**, except that L3 (394 mg, 0.44 mmol) was used in place of L1 in the substitution reaction and dichloromethane/acetone (10:1 v/v) was used as eluent in the column chromatography. Slow diffusion of diethyl ether vapor into a concentrated acetone solution of the complex gave **3**, isolated as a yellow powder. Yield: 271 mg, 0.23 mmol; 55 %. ^{1}H NMR (400 MHz, CD_2Cl_2, 298 K): δ = 1.34 (s, 12H; –Me), 2.75 (s, 6H; –NMe), 5.46 (s, 4H; –OCH_2– on bpy), 6.56 (d, J = 7.7 Hz, 2H; indolinic proton at 7-position), 6.87–6.92 (m, 4H; naphthoxazinic proton at 5′-position and indolinic proton at 5-position), 7.07 (d, J = 7.2 Hz, 2H; indolinic proton at 4-position), 7.19–7.23 (m, 4H; naphthoxazinic proton at 8′-position and indolinic proton at 6-position), 7.61 (d, J = 8.8 Hz, 2H; naphthoxazinic proton at 6′-position), 7.66 (d, J = 5.6 Hz, 2H; bipyridyl proton at 5,5′-position), 7.71–7.74 (m, 4H; naphthoxazinic proton at 7′-position), 7.98 (d, J = 2.5 Hz, 2H; naphthoxazinic proton at 10′-position), 8.41 (s, 2H; naphthoxazinic proton at 2′-position), 9.06 ppm (d, J = 5.6 Hz, 2H; bipyridyl proton at 6,6′-position); IR (KBr disc): $\tilde{\nu}$ = 1896, 1919, 2023 cm^{-1} (C≡O); positive ion FAB-MS: m/z: 1176 $[M+H]^+$, 1140 $[M-Cl]^+$; elemental analyses calcd (%) for $C_{59}H_{48}ClN_6O_7Re\cdot 1/2\,CH_2Cl_2$ (1217): C 58.71, H 4.03, N 6.90; found: C 58.88, H 4.04, N 6.95.

[Re(CO)$_3$(L4)Cl] (4): The title complex was synthesized by a procedure similar to that used for **1**, except that L4 (238 mg, 0.44 mmol) was used in place of L1 in the substitution reaction and chloroform/acetone (2:1 v/v) was used as eluent in the column chromatography. Slow diffusion of diethyl ether vapor into a concentrated acetone solution of the complex gave **4**, isolated as a yellow powder. Yield: 209 mg, 0.25 mmol; 60 %. ^{1}H NMR (400 MHz, CD_2Cl_2, 298 K): δ = 1.36 (s, 6H; –Me), 2.60 (s, 3H; –Me on bpy), 2.77 (s, 3H; –NMe), 5.45 (s, 2H; –OCH_2– on bpy), 6.58 (d, J = 7.7 Hz, 1H; indolinic proton at 7-position), 6.89–6.94 (m, 2H; naphthoxazinic proton at 5′-position and indolinic proton at 5-position), 7.09 (d, J = 6.6 Hz, 1H; indolinic proton at 4-position), 7.18–7.25 (m, 2H; naphthoxazinic proton at 8′-position, indolinic proton at 6-position), 7.36 (d, J = 5.6 Hz, 1H; bipyridyl proton at 5′-position), 7.61–7.65 (m, 2H; naphthoxazinic proton at 6′-position and bipyridyl proton at 5-position), 7.73–7.75 (m, 2H; naphthoxazinic proton at 2′,7′-position), 7.98 (d, J = 2.4 Hz, 1H; naphthoxazinic proton at 10′-position), 8.06 (s, 1H; bipyridyl proton at 3′-position), 8.35 (s, 1H; bipyridyl proton at 3-position), 8.90 (d, J = 5.6 Hz, 1H; bipyridyl proton at 6′-position), 9.06 ppm (d, J = 5.6 Hz, 1H; bipyridyl proton at 6-position); IR (KBr disc): $\tilde{\nu}$ = 1888, 1913, 2022 cm^{-1} (C≡O); positive ion FAB-MS: m/z: 834 $[M+H]^+$, 798 $[M-Cl]^+$; elemental analyses calcd (%) for $C_{37}H_{30}ClN_4O_5Re\cdot 1/4\,CH_2Cl_2$ (853): C 52.42, H 3.60, N 6.56; found: C 52.40, H 3.59, N 6.32.

Physical measurements and instrumentation: Electronic absorption spectra were recorded on a Hewlett–Packard 8452A diode array spectrophotometer. Steady-state emission and excitation spectra at room temperature and at 77 K were recorded on a Spex Fluorolog-2 Model F 111 fluorescence spectrophotometer. Excited state lifetimes of solution samples were measured with a conventional laser system. The excitation source was the 355 nm output (third harmonic, 8 ns) of a Spectra-Physics Quanta-Ray Q-switched GCR-150 pulsed Nd-YAG laser (10 Hz). Luminescence decay traces were recorded on a Tektronix Model TDS 620A digital oscilloscope and the lifetime (τ) determination was accomplished by single exponential fitting of the luminescence decay traces with the model $I(t) = I_o \exp(-t/\tau)$, where $I(t)$ and I_o stand for the luminescence intensities at time = t and time = 0, respectively. Solution samples for luminescence lifetime measurements were degassed by use of at least four freeze-pump-thaw cycles. ^{1}H NMR spectra were recorded on Bruker DPX 300 (300 MHz), Bruker DPX 400 (400 MHz) or Bruker DRX 500 (500 MHz) FT-NMR spectrometers. Chemical shifts (δ, ppm) are reported relative to tetramethylsilane (Me_4Si). All positive ion FAB mass spectra were recorded on a Finnigan MAT95 mass spectrometer. Elemental analyses of all the metal complexes were performed on a Carlo Erba 1106 elemental analyzer by the Institute of Chemistry at the Chinese Academy of Sciences in Beijing.

The thermal bleaching reaction of spirooxazines is known to follow first-order kinetics at various temperatures. The kinetics for the bleaching reaction were determined by measurement of the UV/Vis spectral changes at various temperatures by use of a Hewlett–Packard 8452A diode array spectrophotometer, with temperature controlled by a Lauda RM6 compact low-temperature thermostat. The first-order rate constants were obtained by taking the negative value of the slope of a linear least-squares fit of $\ln[(A-A_\infty)/(A_o-A_\infty)]$ against time according to Equation (1),

$$\ln[(A-A_\infty)/(A_0-A_\infty)] = -kt \quad (1)$$

where A, A_o, and A_∞ are the absorbances at the absorption wavelength maximum of the photomerocyanine at times t, 0, and infinity, respectively and k is the rate constant of the reaction.

The kinetics parameters were obtained by a linear least-squares fitting of $\ln(k/T)$ against $1/T$ according to the linear expression of the Eyring equation (2),

$$\ln(k/T) = -(\Delta H^{\neq}/R)(1/T) + \ln(k_B\,h^{-1}) + (\Delta S^{\neq}/R) \quad (2)$$

where $\Delta H^{\neq}$ and $\Delta S^{\neq}$ are the changes in activation enthalpy and entropy, respectively, T is the temperature, and k_B, R and h are Boltzmann's constant, the universal gas constant and the Planck constant, respectively.

The photochemical quantum yields of the photochromic forward reaction were obtained by a linear least-squares fitting of Equation (3),

$$\phi = \frac{[kV(A-A_0e^{-kt})]}{[\varepsilon I(1-e^{-kt})]} \quad (3)$$

where ϕ is the photochemical quantum yield, V is the volume of irradiated sample solution, ε is the extinction coefficient of the photomerocyanine, and I is the intensity of the light of excitation in Einsteins per second.

Crystal structure determination: All the experimental details are given in Table 1. Crystals of **1** suitable for X-ray studies were obtained by slow diffusion of *n*-hexane vapor into a dichloromethane solution of **1**. A red crystal of dimensions 0.5×0.3×0.2 mm mounted on a glass capillary was used for data collection at 28°C on a MAR diffractometer with a 300 mm image plate detector with use of graphite-monochromated $Mo_{K\alpha}$ radiation (λ = 0.71073 Å). Data collection was made with 2° oscillation of φ, 300 s exposure time and a scanner distance of 120 mm. The images were collected and interpreted, and intensities were integrated by use of the program DENZO.[26] The structure was solved by direct methods by employment of the SIR-97 program[27] on a PC. Almost all atoms, other than atoms of solvent molecules, were located by direct methods and successive least-squares Fourier cycles. The positions of the other non-hydrogen atoms were found after successful refinement by full-matrix, least-squares by use of the SHELXL-97[28] program on a PC. The methyl groups near both ends of the ligand were disordered due to site symmetry as were the related bound N (N4, N6) and C (C38, C47) atoms. Since C and N atoms have very similar scattering factors, disorder of C and N atoms sharing the same positions were not treated. Instead, their positions were located correspondingly. One crystallographic asymmetric unit consisted of one formula unit: that is, a complex molecule, two solvent

molecules of CH_2Cl_2 and two solvent molecules H_2O. In the final stage of least-squares refinement, the disordered atoms were refined isotropically and the other non-hydrogen atoms were refined anisotropically. H atoms (except those of water molecule) were generated by use of the SHELXL-97[28] program. Positions of H atoms were calculated based on riding mode with thermal parameters equal to 1.2 times that of the associated C atoms. The final difference Fourier map was featureless, with maximum residual peaks and holes of 0.958 and $-0.928\ e\text{Å}^{-3}$, respectively.

Crystals of **2** suitable for X-ray studies were obtained by slow diffusion of diethyl ether vapor into a chloroform solution of **2**. A yellowish orange crystal of dimensions $0.5\times0.2\times0.1$ mm mounted on a glass capillary was used for data collection at 28 °C on a MAR diffractometer with a 300 mm image plate detector with use of graphite-monochromated $Mo_{K\alpha}$ radiation ($\lambda = 0.71073$ Å). Data collection was made with 2° oscillation of φ, 600 s exposure time and a scanner distance of 120 mm. The images were collected and interpreted, and intensities were integrated by use of the DENZO[26] program. The structure was solved by direct methods by employment of the program SIR-97[27] on a PC. Most atoms were located according by direct methods and successive least-square Fourier cycles. The positions of the other non-hydrogen atoms were found after successful refinement by full-matrix, least-squares by use of the SHELXL-97[28] program on a PC. One crystallographic asymmetric unit consisted of one formula unit: that is, a complex molecule, with one solvent molecule of $CHCl_3$. In the final stage of least-squares refinement, all non-hydrogen atoms were refined anisotropically. H atoms were generated by use of the SHELXL-97[28] program. The positions of H atoms were calculated based on riding mode with thermal parameters equal to 1.2 times those of the associated C atoms. The final difference Fourier map was featureless, with maximum residual peaks and holes of 0.563 and $-1.004\ e\text{Å}^{-3}$, respectively.

CCDC-218382 (**1**) and CCDC-218383 (**2**) contain the supplementary crystallographic data for this paper. These data can be obtained free of charge via www.ccdc.cam.ac.uk/conts/retrieving.html (or from the Cambridge Crystallographic Data Centre, 12 Union Road, Cambridge CB2 1EZ, UK; fax: (+44) 1223-336033; or deposit@ccdc.cam.ac.uk).

Acknowledgement

V. W.-W. Y. acknowledges support from The University of Hong Kong Foundation for Educational Development and Research Limited and The University of Hong Kong. The work described in this paper was supported by the Research Grants Council of the Hong Kong Special Administrative Region, China (Project HKU7097/01P). C.-C. K. acknowledges the receipt of a Croucher Scholarship from the Croucher Foundation and a Li Po Chun Postgraduate Scholarship from Li Po Chun Charitable Fund, and K. M.-C. W. and N. Z. the receipt of University Postdoctoral Fellowships from The University of Hong Kong.

[1] a) S. Seikosha Co. , *Jap. Pat.* **1984**, *978*(5), 721; b) C. Salemi-Delvaux, B. Luccioni-Houze, G. Baillet, G. Giusti, R. Guglielmetti, *J. Photochem. Photobiol. A* **1995**, *91*, 223.

[2] J. Malkin, A. S. Dvornikov, K. D. Straub, P. M. Rentzepis, *Res. Chem. Intermed.* **1993**, *19*, 159.

[3] a) S. Yitzchaik, G. Berkovic, V. Krongauz, *Chem. Mater.* **1990**, *2*, 168; b) N. Tamaoki, E. Van Keuren, H. Matsuda, K. Hasegawa, T. Yamaoka, *Appl. Phys. Lett.* **1996**, *69*, 1188.

[4] a) I. Willner, S. Rubin, R. Shatzmiller, T. Zor, *J. Am. Chem. Soc.* **1993**, *115*, 8690; b) M. L. Dagan, E. Katz, I. Willner, *J. Chem. Soc. Chem. Commun.* **1994**, 2741; c) I. Willner, B. Willner, *Adv. Mater.* **1995**, *7*, 587; d) R. Blonder, E. Katz, I. Willner, V. Wray, A. F. Bückmann, *J. Am. Chem. Soc.* **1997**, *119*, 11747; e) I. Willner, *Acc. Chem. Res.* **1997**, *30*, 347; f) A. N. Shipway, I. Willner, *Acc. Chem. Res.* **2001**, *34*, 421.

[5] a) H. Shinmori, M. Takeuchi, S. Shinkai, *J. Chem. Soc. Perkin Trans. 2* **1996**, 1; b) M. Inouye, M. Ueno, T. Kitao, *J. Am. Chem. Soc.* **1990**, *112*, 8977c) M. Inouye, Y. Noguchi, K. Isagawa, *Angew. Chem.* **1994**, *106*, 1226; *Angew. Chem. Int. Ed. Engl.* **1994**, *33*, 1163; c) M. Inouye, *Coord. Chem. Rev.* **1996**, *148*, 265; d) M. Inouye, K. Akamatsu, H. Nakazumi, *J. Am. Chem. Soc.* **1997**, *119*, 9160; e) M. Tanaka, M. Nakamura, M. A. A. Salhin, T. Ikeda, K. Kamada, H. Ando, Y. Shibutani, K. Kimura, *J. Org. Chem.* **2001**, *66*, 1534.

[6] T. Inada, S. Uchida, Y. Yokoyama, *Chem. Lett.* **1997**, *26*, 321.

[7] a) N. Y. C. Chu, *Can. J. Chem.* **1983**, *61*, 300; b) N. Y. C. Chu, in *Photochromism: Molecules and Systems* (Eds.: H. Dürr, T. H. Bouas-Laurent), Elsevier, Amsterdam, **1990**, p. 879.

[8] a) J. C. Crano, R. Guglielmetti, *Organic Photochromic and Thermochromic Compounds*, Plenum Press, New York, vols. 1 and 2, **1999**; b) G. Berkovic, V. Krongauz, V. Weiss, *Chem. Rev.* **2000**, *100*, 1741.

[9] a) M. Querol, B. Bozic, N. Salluce, P. Belser, *Polyhedron* **2003**, *22*, 655; b) J. L. Bahr, G. Kodis, L. Garza, S. Lin, A. L. Moore, T. A. Moore, D. Gust, *J. Am. Chem. Soc.* **2001**, *123*, 7124; c) V. W. W. Yam, C. C. Ko, L. X. Wu, K. M. C. Wong, K. K. Cheung, *Organometallics* **2000**, *19*, 1820; d) R. F. Khairutdinov, K. Giertz, J. K. Hurst, E. N. Voloshina, N. A. Voloshin, V. I. Minkin, *J. Am. Chem. Soc.* **1998**, *120*, 12707.

[10] A. R. Oki, R. J. Morgan, *Synth. Commun.* **1995**, *25*, 4093.

[11] D. G. McCafferty, B. M. Bishop, C. G. Wall, S. G. Hughes, *Tetrahedron* **1995**, *51*, 1093.

[12] S. Gould, G. F. Strouse, T. J. Meyer, B. P. Sullivan, *Inorg. Chem.* **1991**, *30*, 2942.

[13] a) E. Horn, M. R. Snow, *Aust. J. Chem.* **1980**, *33*, 2369; b) P. Chen, M. Curry, T. J. Meyer, *Inorg. Chem.* **1989**, *28*, 2271; c) V. W. W. Yam, V. C. Y. Lau, K. K. Cheung, *J. Chem. Soc. Chem. Commun.* **1995**, 259; d) V. W. W. Yam, K. M. C. Wong, V. W. M. Lee, K. K. W. Lo, K. K. Cheung, *Organometallics* **1995**, *14*, 4034; e) V. W. W. Yam, V. C. Y. Lau, K. K. Cheung, *Organometallics* **1996**, *15*, 1740; f) V. W. W. Yam, K. Z. Wang, C. R. Wang, Y. Yang, K. K. Cheung, *Organometallics* **1998**, *17*, 2440; h) V. W. W. Yam, S. H. F. Chong, K. K. Cheung, *Chem. Commun.* **1998**, 2121; i) V. W. W. Yam, S. H. F. Chong, C. C. Ko, K. K. Cheung, *Organometallics* **2000**, *19*, 5092.

[14] a) E. Miler-Srenger, R. Guglielmetti, *Acta Crystallogr. Sect. C* **1984**, *40*, 2050; b) J. C. A. Boeyens, *J. Cryst. Mol. Struct.* **1978**, *8*, 317; c) R. Millini, G. D. Piero, P. Allegrini, L. Crisci, V. Malatesta, *Acta Crystallogr. Sect. C* **1991**, *47*, 2567; d) W. Clegg, N. C. Norman, J. G. Lasch, W. S. Kwak, *Acta Crystallogr. Sect. C* **1987**, *43*, 1222; e) J. Crano, D. Knowles, P. Kwiatkowski, T. Flood, R. Ross, L. Chiang, J. Lasch, R. Chadha, C. Siuzdak, *Acta Crystallogr. Sect. B* **1994**, *50*, 772; f) K. Chamontin, V. Lokshin, R. Guglielmetti, A. Samat, G. Pèpe, *Acta Crystallogr. Sect. C* **1998**, *54*, 670.

[15] G. Favaro, F. Masetti, U. Mazzucato, G. Ottavi, P. Allegrini, V. Malatesta, *J. Chem. Soc. Faraday Trans.* **1994**, *90*, 333.

[16] a) M. S. Wrighton, D. L. Morse, *J. Am. Chem. Soc.* **1974**, *96*, 998; b) J. C. Luong, H. Faltynak, M. S. Wrighton, *J. Am. Chem. Soc.* **1979**, *101*, 1597; c) S. M. Fredericks, J. C. Luong, M. S. Wrighton, *J. Am. Chem. Soc.* **1979**, *101*, 7415; d) P. J. Giordano, M. S. Wrighton, *J. Am. Chem. Soc.* **1979**, *101*, 2888; e) J. V. Caspar, T. J. Meyer, *J. Phys. Chem.* **1983**, *87*, 952.

[17] a) H. Görner, A. K. Chibisov, *J. Chem. Soc. Faraday Trans.* **1998**, *94*, 2557; b) J.-L. Pozzo, A. Samat, R. Guglielmetti, D. Keukeleire, *J. Chem. Soc. Perkin Trans. 2* **1993**, 1327.

[18] a) D. Eloy, P. Escaffre, R. Gautron, P. Jardon, *J. Chim. Phys.* **1992**, *89*, 897; b) G. Favaro, V. Malatesta, C. Miliani, A. Romani, *J. Photochem. Photobiol. A* **1996**, *97*, 45; c) J. Hobley, F. Wilkinson, *J. Chem. Soc. Faraday Trans.* **1996**, *92*, 1323.

[19] a) A. K. Chibisov, H. Görner, *J. Phys. Chem. A* **1999**, *103*, 5211; b) A. K. Chibisov, H. Görner, *Phys. Chem. Chem. Phys.* **2001**, *3*, 424.

[20] M. Campredon, G. Giusti, R. Guglielmetti A. Samat, G. Gronchi, A. Alberti, M. Benaglia, *J. Chem. Soc. Perkin Trans. 2* **1993**, 2089.

[21] A. Alberti, C. Barberis, M. Campredon, G. Gronchi, M. Guerra, *J. Phys. Chem.* **1995**, *99*, 15779.

[22] a) J. C. Luong, L. Nadjo, M. S. Wrighton, *J. Am. Chem. Soc.* **1978**, *100*, 5790; b) C. Kutal, M. A. Weber, G. Ferraudi, D. Geiger, *Organometallics* **1985**, *4*, 2161; c) J. Hawecker, J. M. Lehn, R. Ziessel, *Helv. Chim. Acta* **1986**, *69*, 1990; d) K. Kalyanasundaram, *J. Chem. Soc. Faraday Trans. 2* **1986**, *82*, 2401; e) B. J. Yoblinski, M. Stathis, T. F. Guarr, *Inorg. Chem.* **1992**, *31*, 5.

[23] a) M. Hosoda, *Eur. Pat. Appl.* EP 186364 A2, July 2, **1986**. b) B. Osterby, R. D. McKelvey, L. Hill, *J. Chem. Educ.* **1991**, *68*, 424.

[24] a) J. V. Caspar, B. P. Sullivan, T. J. Meyer, *Inorg. Chem.* **1984**, *23*, 2104; b) B. P. Sullivan, T. J. Meyer, *J. Chem. Soc. Chem. Commun.* **1984**, 403.
[25] Derivation of Equation 3, please refer to Supporting Information.
[26] DENZO (version 1.3.0): "*The HKL Manual - A description of programs DENZO, XDISPLAYF, and SCALEPACK*" written by D. Gewirth, with the co-operation of the program authors Z. Otwinowski, W. Minor, (**1995**), Yale University, New Haven, U.S.A.
[27] Sir97: a new tool for crystal structure determination and refinement, A. Altomare, M. C. Burla, M. Camalli, G. Cascarano, C. Giacovazzo, A. Guagliardi, A. G. G. Moliterni, G. Polidori, R. Spagna, *J. Appl. Cryst.*, **1998**, *32*, 115.
[28] SHELXS-97, G. M. Sheldrick, (**1997**). SHELX-97: Programs for Crystal Structure Analysis (Release 97–2). University of Göttingen, Germany.

Received: August 27, 2003 [F5485]